6 January 1978, Volume 199, Number 4324 **SCIENCE**

Structure and Properties of Metallic Glasses

P. Chaudhari and D. Turnbull

Summary. Recent experience has shown that certain metal alloys can be put into glass form by rapid melt-quenching or by various condensation processes. Models for the nature and structure of these glasses are surveyed and shown to be quite parallel to those already developed for the more common nonmetallic glasses. The rather unique magnetic, superconducting, and mechanical properties and the technical potential of metallic glasses are also discussed.

Traditionally, glasses are defined as bodies formed by the continuous hardening or solidification of a liquid. Diffraction examinations have always proved them to be structurally amorphous, by which we mean that any translational correlations in the equilibrium positions of the constituent molecules die out within distances of a few molecular diameters. Amorphous solid bodies also may form by various discontinuous condensation processes from fluids, either gas or liquid, which are highly dilute in the solidifying constituent. Often there is no discernible difference between the molecular configurations in an amorphous solid formed by condensation and one formed by liquid solidification. Consequently, despite vigorous objections of glass technologists, the terms glassy and amorphous solid states are often used interchangeably.

The glasses with which we are most familiar are nonmetallic and silicate-based. They have been most noteworthy technologically, over many centuries, for their extraordinary transparency to radiation in the visible range. A substantial part of their cohesion is due to highly directed covalent bonds.

Recent experience has extended greatly the number and chemical variety of materials which have been put into amorphous solid form and has indicated that directed covalency is not as important a condition for glass formation as had been supposed. Thus many simple molecular substances, such as toluene, are now included among the glass formers. More remarkably, some of the most recent experience has shown that certain metal alloys, in which directed covalency must be minimal, can be put into amorphous solid form by condensation or melt solidification.

These findings have again, and more forcefully, directed attention to the problem of what uniquely distinguishes the amorphous solid state, in its many manifestations, from the crystalline and fluid states of matter. In this article we present a perspective on this problem. We then discuss the striking and quite unique electrical, magnetic, and mechanical behavior of some of the newly discovered glassy metals from this perspective. We have not attempted a comprehensive survey of the now extensive literature on glassy metals, much of which is discussed, from various viewpoints, in several recent reviews (*1–10*).

Distinguishing Characteristics

Macroscopically, amorphous and crystalline solids are distinguished from fluids by their resistance to shape change or flow, usually specified by the magnitude of the shear viscosity, η. The flow resistance of materials under various conditions exhibits a continuum of values, so the choice of the upper limit of the viscosity of the fluid range is arbitrary. Practically (*11*), this limit is usually taken to be $\eta \sim 10^{15}$ poise; at this viscosity a body would substantially maintain its shape against small shearing forces for periods up to 1 day. For reference, at room temperature the viscosities of many common liquids, such as water, ethyl alcohol, and mercury, are near 10^{-2} poise.

Microscopically, a somewhat sharper distinction between solids and fluids can be made in terms of the nature of the motions of the constituent molecules. The motions are wholly oscillatory in the ideal solid, while in fluids they are in substantial part (wholly in the ideal limit) translatory. This means that in a solid there exists, during the periods of observation, a well-defined set of equilibrium positions about which the molecules oscillate. The fluid exhibits no such set of positions, and its structure must be characterized in terms of a most probable configuration of molecular positions relative to that of a moving reference molecule.

The equilibrium positions in the crystalline solid, in contrast with those in the amorphous solid, are correlated translationally over many molecular spacings. To compare the configurations of equilibrium positions in crystalline and amorphous solids it is important to specify certain elements of the short-range order (SRO). These include the number, z, of immediate neighbors and the separations, r_z, of these neighbors from the reference molecule. Also, since the SRO can exhibit essentially different topologies even with the same values for both z and r_z, the angular distributions of the near neighbors must be given. This characterization of the SRO is provided most conveniently by the Voronoi or, more familiarly, the Wigner-Seitz (W-S) construction. This construction is made by passing perpendicularly bisecting planes

---

P. Chaudhari is the manager of the Department of Thin-Film Physics, IBM Thomas J. Watson Research Center, Yorktown Heights, New York 10598, and D. Turnbull is Gordon McKay professor of applied physics, Harvard University, Cambridge Massachusetts 02139.

0036-8075/78/0106-0011$02.00/0

through each line connecting the center of the reference molecule to the center of every other molecule in the body. The innermost polyhedron so formed is usually known as the W-S cell. Its faces and the lengths of the lines which they bisect define, respectively, z, and r_z values. The topology of the SRO is specified by the shape of the cell.

We may choose a molecular unit, or basis, consisting of one or more atoms, in the crystal such that the W-S polyhedra are identical for all units. In contrast, the W-S polyhedra of an amorphous solid, however the basis is chosen, will vary in form and size. We shall see that the average values of z and r_z of amorphous solids, as defined by the W-S construction, are fairly well established. The major controversies concerning amorphous solid structure and its relation to crystal structure center on the topology of its SRO.

Thermodynamic Characterization

It is well established that materials are more stable in some crystallized state, single or polyphase, than in their amorphous solid forms. Further, all amorphous solids tend to relax toward lower-energy amorphous states by slow molecular rearrangements which, in contrast to the heterogeneous crystallization processes, occur homogeneously. The time constants, τ_c, for molecular rearrangements in glass-forming liquids scale roughly as the shear viscosity, such that, for example, $\tau_c \sim 1$ day at the solidification point, where $\eta \sim 10^{15}$ poise. At this point η and τ_c are increasing sharply with decreasing temperature, typically by a factor of 2 to 3 per degrees Celsius. From this behavior it is apparent (*12*) that at only a few degrees below the solidification point τ_c becomes so large that the amorphous solid will not, in practice, reach configurational equilibrium but will be "frozen" in a single configuration. Thus the amorphous solid state, although its SRO may be topologically unique, is thermodynamically neither stable nor well defined. However, an isolated amorphous solid will persist in its configurationally frozen state without crystallizing for all periods over which observation is practical.

During configurational freezing the heat capacity, C_p, of the melt usually drops sharply (see Fig. 1) to levels near those of the crystallized system (*12*). This drop reflects only the loss of the configurational freedom, and the slower the cooling, the lower the temperatures at which it occurs. At normal cooling rates (for example, 10^{-2} °C per second) the range of temperatures centers at the value, called the glass temperature, T_g, at which $\eta \sim 10^{13}$ poise. The magnitude of the drop in C_p at the melt $\rightarrow$ glass transition is large (for example, 50 percent) for most glass formers, but it is hardly detectable (*13, 14*) in the tetrahedrally coordinated systems SiO_2 and GeO_2. The occurrence of configurational freezing is not limited to glass formation. For example, a crystalline alloy which is compositionally disordered is frozen into a particular configuration at low temperatures, where interatomic positional exchanges are practically precluded by the high kinetic resistance to them. However, the thermal manifestation of this freezing is not nearly so striking as in the glass transition, since the temperature dependence of atomic transport in crystalline alloys is generally much smaller than that of τ_c at the glass transition.

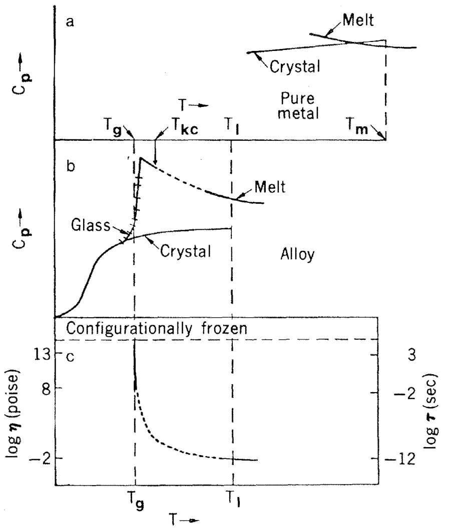

Fig. 1. Idealized representation (*26, 27*) of rheological and thermal manifestation of the melt $\leftarrow\rightarrow$ glass transition in metal alloys. (a) Temperature dependence of the heat capacity of the pure host metal in its liquid and crystalline forms near the thermodynamic melting temperature, T_m. (b) Dependence of the heat capacity on the temperature of the same alloy in its several states. (c) Dependence of the shear viscosity and the time constant for flow of a glass-forming molten alloy on temperature.

In contrast to its behavior in the glass transition range, τ_c is usually quite small and only increases slowly with falling temperature at and just below the thermodynamic crystallization temperature, T_m. The several models (*15–19*) advanced to account for the sharply increasing dependence of τ_c on T (see Fig. 1) as T_g is approached are all based on the concept that molecular rearrangement in the melt requires a highly correlated set of molecular motions.

Despite the rapidity with which they come to configurational equilibrium at $T > T_g$, most melts, when not in contact with extraneous crystals, exhibit extraordinarily high resistance to crystal nucleation to temperatures far below T_m (for example, to 0.75 T_m, or, for many glass formers, to all T). In this undercooled regime the melt is in a well-defined metastable state in which configurational equilibrium is virtually maintained. The heat capacity change, ΔC_p, for the crystal $\rightarrow$ melt transition is positive and, indeed, increases with undercooling. Thus, the entropy of melting, ΔS_m, continually decreases with increasing undercooling to the configurational freezing point. Kauzman (*12*) documented this trend and noted that if it continued into the temperature range below T_g, ΔS_m for many systems would go to zero at temperatures well above 0°K. This behavior implies that if configurational equilibrium could be maintained below T_g, the amorphous system would undergo a continuous transition to a solid with negligible configurational entropy. The configuration of this hypothetical solid is a major problem for the theory of the glass state. Kauzman thought that it must be crystalline, which would mean that a continuous transition from the amorphous to the crystalline state is possible. Opposed to this is the view that the system is tending toward an "ideal" amorphous solid state, in internal equilibrium, characterized by an SRO which is topologically unique and distinct from that of crystals. A structural basis for this concept was first provided by Zachariasen's random network model (*20*), described in a later section, for amorphous solids. Later, Gibbs and DiMarzio (*21*) provided a statistical basis for understanding how the configurational entropy might virtually disappear in the formation of an ideal amorphous solid.

The main features of the thermal and crystallization behavior just outlined are exhibited by metallic as well as by nonmetallic melts. While $C_p(T)$ follows a downward course with rising T for most pure metal melts (*22*), it intersects the $C_p(T)$ curve for the corresponding crystal at a temperature, T_l, which ranges, depending on the metal, from 0.9 to 1.1 T_m. As T falls below T_l, ΔC_p is positive and increasing so that ΔS_m is decreasing. This trend continues in the undercooled range as far as measurements have been extended. Thus the problem of the nature of a state of very low configurational entropy approached continuously from the melt arises for metals as well as nonmetals.

Pure metal melts can sustain undercoolings of 0.2 to 0.3 T_m for long periods without crystallization even though crystallization fronts, when formed by seeding or homogeneous (unseeded) nucleation, move at extremely high speeds (up to 100 meters per second) (*23*). This behavior suggested that crystal nucleation results only from configurations which require substantial topological reconstruction of the SRO of the melt and which, therefore, rarely occur. On this basis, Cohen and Turnbull (*15, 24*) predicted that an ideal amorphous solid state of monatomic systems should exist.

When quenched at the highest available rates to temperatures below 0.7 T_m, pure molten metals have always crystallized. This behavior probably reflects the occurrence of copious homogeneous nucleation of crystals at $T \lessdot 0.7\ T_m$ and the fact that the T_g's of pure metal lie far below 0.7 T_m. However, beginning with the experiments of Duwez and associates (*25*), a number of metallic alloys have been melt-quenched to amorphous solid form. Chen and Turnbull (*26, 27*) demonstrated that at least some of these alloys exhibit both the thermal and rheological manifestations of the melt $\longleftrightarrow$ glass transition typical of glass formers (see the schematic representation of transition behavior in Fig. 1). These are the developments which established that metals can form "proper" glasses and stimulated a broader perspective on the nature of the glass state.

Structure of Amorphous Solids

We have noted that the central problem of amorphous solid structure is to fully characterize its SRO and to establish the topological rules which determine it. The oldest and most frequently used method of partly achieving this characterization is by Fourier inversion of the x-ray, electron, or neutron radiation diffracted by the solid, which gives information on its average atomic arrangement. This method was introduced by F. Zernike and J. A. Prins in 1927 and is described in detail in many publications; for example, see the book by Warren (*28*) or Cargill's review (*7*).

This Fourier inversion of diffraction data yields the radial distribution function (RDF) $4\pi r^2 \rho(r) dr$, where $\rho(r)$ is the average density of atoms at distance r from a reference atom. At large $r, \rho(r)$ approaches the average density, ρ_0, of the solid as a whole. A typical experimentally determined RDF, for amorphous germanium (*29*), which is a semiconductor, and the pair distribution function $\rho(r)/\rho_0$ for a nickel-phosphorus alloy (*7*), which is metallic, are shown in Figs. 2 and 3. The first peak in the RDF occurs at the most probable position of nearest-neighbor atoms, and the area under it gives the coordination number at this position—that is, the average number of nearest neighbors of the reference atom. Such data have shown that the number of nearest neighbors, z, of an atom in amorphous semiconducting silicon or germanium is 4, as in the crystalline form of these elements; this result reflects the strong covalent bonding in these materials. Similar analyses indicate that $z \approx 12$

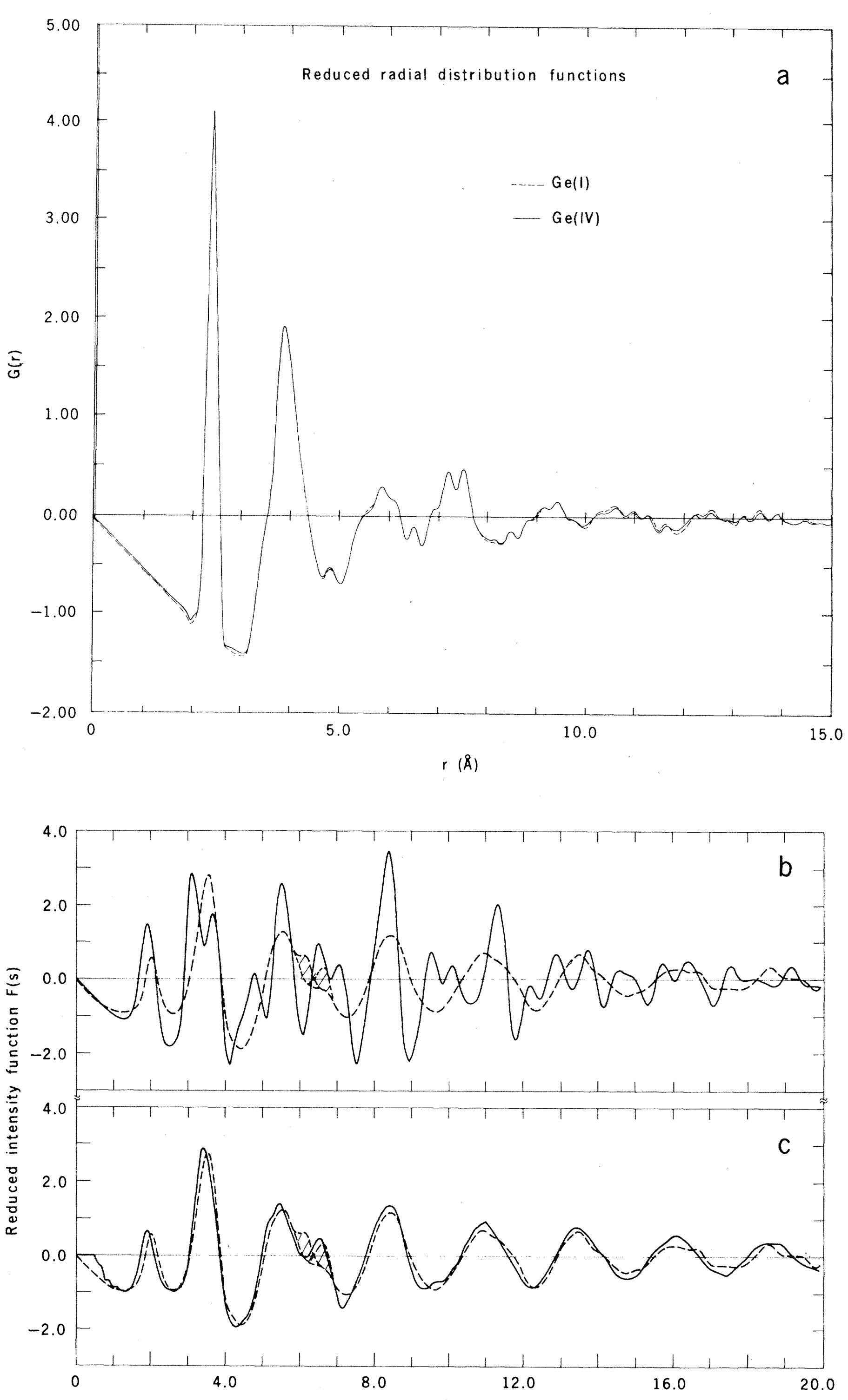

Fig. 2. (a) Reduced radial distribution function for amorphous germanium prepared by evaporation (Ge I) and by ion implantation (Ge IV) of an initially polycrystalline film (*29*). (b and c) Comparison of experimental (dashed curve) and calculated (solid curve) reduced intensity functions for amorphous germanium. (b) Amorphous germanium and microcrystallite (diamond cubic) model. (c) Amorphous germanium and random network model (*29*). (This function is related to the radial distribution function described in the text through a Fourier transform.)

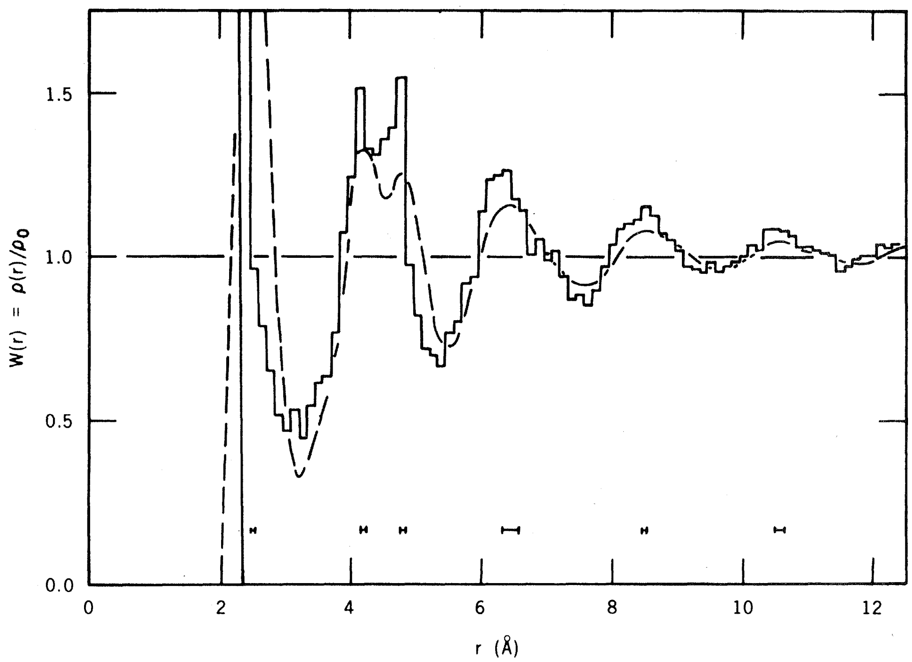

Fig. 3. Pair distribution function for an amorphous cobalt-phosphorous alloy. The dashed line represents experimental data; the histogram was calculated by using the DRP model (*37*).

in most amorphous metallic solids, compared with $z = 12$ or 8 in the close-packed or body-centered cubic, respectively, crystalline forms of the constitutent metals. The RDF's also show clearly that positional correlations in amorphous solids remain perceptible only to distances of about five atomic diameters, or ~ 15 angstroms.

Since it represents only the positional dependence of the average atomic density, the RDF does not establish a unique set of coordinates of the atomic positions, from which the topology of the SRO could be deduced. However, although it does not tell us what the structure is, the RDF can, in conjunction with the macroscopic density, tell us what the structure is not; that is, we may calculate the RDF for any proposed structural model and determine its consistency with the experimental RDF.

The structural models used in attempts to account for the RDF's of amorphous solids range from the microcrystallite to the continuous random type. Proposed microcrystalline models are usually assemblies of misoriented microcrystals with diameters averaging five to ten atomic spacings. In the testing of these models the problem of intercrystallite connectivity—that is, the configurations in intercrystalline regions and the spatial correlations of the crystallite orientations—is rarely dealt with directly and most often is entirely ignored. Usually it is tacitly assumed that the spatial orientations of the crystallites are completely uncorrelated. The second, continuous random, class of model has as its essential structural elements configurations which by themselves are noncrystallographic. One such configuration is a regular tetrahedral arrangement of atoms which can be incorporated into periodic space-filling arrangements only when combined with other kinds of configurations.

The earliest continuous-type model was the random network proposed by Zachariasen (*20*) and applied to covalently bound glasses. In such a structure the full interatomic connectivity is maintained but with substantial dispersion of bond angles about some average value. Physical models of random networks may be constructed by using some bond angle dispersion relation, and the RDF may then be computed from the actual positions of the network nodes. For example, a network of this type was handbuilt by Polk (*30*) to model the structures of the amorphous 4-coordinated elemental solids silicon and germanium. It is found that the diffraction data and RDF's of amorphous covalent solids are generally well fit by the random network models (*29*) (see Fig. 2c). In contrast, the fits obtained with the microcrystallite models, supposing no correlations in the spatial orientations of crystallites, are not satisfactory (*7, 29, 31*) (see Fig. 2b).

For centrosymmetrically bonded monatomic systems, the analog to the random network is the structure formed by the densest random packing (DRP) of uniform spheres. Such structures were assembled from hard spheres, which are known to model real monatomic systems surprisingly well [for example, see Rice (*32*)], and characterized by Bernal (*33*) and Finney (*34*). Perhaps the most conspicuous feature of the DRP structure is the prevalence of configurations in which the centers of four contacting spheres form tetrahedra with nearly regular shapes. This tetrahedral motif permits transformation of the DRP structure into the 4-coordinated random network structure for silicon or germanium, in which atoms occupy centers as well as vertices of distorted tetrahedra, and vice versa. This transformation is nonconservative and is effected by addition, or removal, of an atom at the center of each tetrahedron (*35*).

Cohen and Turnbull (*24*) suggested that the DRP structure should model that of ideal monatomic glasses, and later Cargill (*36, 37*) showed that his diffraction results for a nickel-based nickel-phosphorous amorphous alloy were well fit by the structure. Several modifications to these ideas have been made in recent years, including the use of two sphere diameters to describe the structure of alloys (*38*). A further important feature of the recent model studies (*39, 40*) has been the use of soft, in contrast to hard-sphere, repulsive potentials.

Both dense random packed and random network model structures are constructed on the basis of a single algorithm which is applicable at all stages of the building of the model. In contrast to such continuous random modeling, an amorphous solid might be formed by small and ordered, but noncrystalline, clusters. The motivation for forming this, as well as the DRP, structure may derive from energetic preference, under the operation of centrosymmetric short-range interatomic forces, for tetrahedral configurations of the type described above. Of the arrangements in which all atoms are located at vertices of regular polyhedra, it is the tetrahedral one which has the highest density per atom. We might suppose that the assemblies of lowest potential energy would be those composed entirely by regular tetrahedral arrangements, but space cannot be wholly filled by the stacking of regular tetrahedra alone. To form a crystalline closed-packed structure, presumably the highest-density structure of an infinite number of uniform hard spheres, it is necessary to include the less dense and more energetic octahedral configurations in the ratio of one per two tetrahedra. However, in assembling a small, in contrast to an infinite, number of atoms, the tetrahedral motif, with small distortions of the tetrahedra from regularity, can be much more prominent. Indeed, Frank (*41*) showed that 13 atoms assembled by

Lennard-Jones forces should have a lower potential energy in an icosahedral arrangement, in which 20 slightly distorted tetrahedra are stacked together from a central point, than in either of the close-packed crystalline arrangements. The icosahedral configuration exhibits fivefold symmetry and so cannot by itself constitute a crystalline unit cell. It can be incorporated into crystalline arrangements only by combination with other larger polyhedra, as in Frank-Kasper (*42*) phases.

Recently there have been calculations (*43, 44*) of the relative potential energies of larger clusters of atoms in various arrangements, again assembled by Lennard-Jones forces. Hoare and Pal (*43*) showed that, in assemblies of up to 50 atoms, certain noncrystalline arrangements, essentially formed by distorted tetrahedra, are more stable than the close-packed crystalline ones. These developments suggested that the monatomic amorphous solid might consist of some combination of such polytetrahedra. Analog models for covalently bound systems, Tilton's (*45*) "vitron" and Grigorivici and Manaila's (*46*) "amorphon," had been proposed earlier. Some support for the amorphous cluster model for monatomic systems is provided by the finding of Farges *et al.* (*47*) that small argon clusters, containing about 100 atoms, are amorphous as formed in beams ejected from supersonic nozzles. Also, thin films formed by vapor deposition do not usually grow monolayer by monolayer. Instead, the initially deposited material is in the form of small clusters or islands which, as deposition proceeds, grow and coalesce to form a continuous film. It is reasonable to suppose that the initial clusters would have been in the stable noncrystalline arrangements described by Hoare and Pal.

A major unresolved problem with the amorphous cluster models, as with the microcrystallite models, is that of cluster connectivity. Can we connect the largest stable clusters without using such large holes that the cluster assembly will lose its energetic advantage over the continuous DRP structure? It appears that the density of any connected cluster model could hardly exceed that of a Frank-Kasper (*42*) structure of uniform hard spheres. The maximum density of such a structure has not, to our knowledge, been established, but it must be well below that of crystalline close-packing.

It is possible that the amorphous clusters, if optimally connected—that is, to maximize the density of an infinite assembly—would distort into a structure hardly distinguishable from a DRP one. To consider this possibility, we examine the form distribution of polyhedral holes in the DRP structure delineated by the center of near-neighbor atoms. Bernal (*33*) noted that all the holes could be formed by small distortions from five ideal polyhedra ("canonical" holes), each bound entirely by triangular faces. The striking feature of the distribution, which we have already noted, was the high proportion (84 percent) of tetrahedral holes and the paucity (~ 5 percent) of octahedral holes. Thus the structure might be regarded as an assembly of tetrahedral configurations with connectivity provided by inclusion, in small proportion, of the larger holes. This tetrahedral configurations with connectivity provided by inclusion, in small those formed by film deposition on cold substrates or by continuous densification of fluids, governed primarily by short-range centrosymmetric interactions. Indeed, a computer simulation of condensation, in which each incoming atom is fixed at the lowest-energy surface binding site, generates amorphous structures topologically similar to that of DRP (*48, 49*). The high resistance of monatomic melts to crystal nucleation, which we have noted, may reflect the fact that fluctuations that transform polytetrahedral to crystal-like configurations rarely occur in these melts.

Further characterization of the structure of amorphous solids has been achieved by application of various spectroscopic techniques. Generally these studies have confirmed the high degree of development of SRO in amorphous solids, but so far they have added little information on the SRO topology.

It appears that high-resolution electron microscopy should reveal important details on atomic configurations in thin amorphous films. Indeed, it had been thought that dark-field transmission microscopy (*50, 51*), in conjunction with interference micrographs (*50, 52*), indicated microcrystallinity in amorphous germanium and silicon films. However, when care was taken (*53*) to eliminate artifacts, no evidence for such crystallinity was found, although planar atomic alignments were observed. Further, electron transmission microscopy, as well as diffraction from minute volumes (*54*), of similar films gave no indications of ordered clusters of microcrystallinity at resolutions of about four atomic spacings.

The occurrence in amorphous solids of highly localized (scale ~ 10 Å) anisotropies, due to chance atomic alignments, is to be expected. Indeed, Chaudhari and associates have demonstrated the existence of such alignments extending for several atomic diameters in amorphous films (*53*), by electron microscopy, and in both random network and DRP models (*55*).

Chaudhari *et al.* (*56*) also found, by measurements of magnetic properties, some quite unexpected long-range anisotropies in certain amorphous films. It is believed that these anisotropies may arise during film formation because of the directionalities of the deposition process or of cooling. Indeed, a computer simulation (*57*) of a film deposition generated such an anisotropy by the self-shadowing effect of the deposited atoms in the oncoming atomic stream. The RDF of the simulated film was as expected for an amorphous solid, but the number of atomic pairs in directions orthogonal to and within the plane of the film were different.

Formation of Amorphous Solids

The main requirement for putting materials into amorphous solid form is to avoid the thermodynamically preferred crystallization processes. The necessary conditions for this avoidance have been described elsewhere (*58–62*). They may be achieved by one of the following general procedures: (i) melt quenching to $T < T_g$, (ii) condensation from a dilute fluid onto a substrate held at $T < T_g$, or (iii) irradiating a crystalline solid at $T < T_g$.

The likelihood that a melt, when free of extraneous crystals, will undercool through its metastable regime, from T_m through T_g, should be greater the higher are the cooling rate and the reduced glass temperature, $T_{rg} = T_g/T_m$, and the smaller is the specimen volume (*59*). Analyses based on simple nucleation theory (*62*) indicate that melts with $T_{rg} \gtrsim 2/3$, if unseeded, should readily form glasses even when large volumes are slowly cooled. Indeed, the T_{rg}'s of the common silica-based and organic glass formers generally exceed 2/3. The lower limiting T_{rg} for glass formation should be reduced substantially by the use of higher quench rates.

Ultrahigh quench rates for molten metals, 10^6°C/sec and higher, were achieved in the "splat" cooling experiments of Duwez and associates (*1, 25*). They succeeded, for the first time, in quenching a molten metal alloy (Au_4Si) to a glass. By means of splat cooling or variant techniques, a considerable number of different alloys have now been quenched to glasses. These glasses have exhibited T_{rg}'s ranging from about 0.6

down to 0.45, in agreement with the simple nucleation theory calculation (*62*), indicating that at cooling rates of 10^6°C/sec glass formation should be possible at all $T_{rg} \gtrsim 0.45$.

The ultrahigh quench rates are achieved, essentially, by driving molten metal onto a cold metal substrate. On impact, the metal spreads into a thin layer, a few micrometers thick, in which the rapid cooling occurs. Methods have now been developed by Allied Chemical (*8*) and other laboratories for producing glassy metals in the form of continuous thin ribbons. In these processes a jet of molten metal is driven continuously onto a rotating metal substrate. The metal is spread into a thin ribbon, which is thrown off the substrate after solidification. The directionality in heat transfer during rapid cooling can lead to differences between the in-plane and transverse properties of the ribbons.

It is evident that certain kinds of alloying greatly facilitate the formation of glassy metals in melt quenching. Actually, it had been established earlier that impurity admixture is essential for producing metals by electrodeposition (*63*) or vapor deposition (*64, 65*) that would persist in amorphous solid form up to and above room temperature. Impurities could strongly retard the crystal growth rates in amorphous solids, especially if growth had to be attended by impurity redistribution. However, the melt-quenching experiments strongly suggest that a major effect of the added impurities that facilitate glass formation is to increase T_{rg}.

Addition of impurities to a host may increase T_{rg} either by raising T_g or by lowering T_m. In the metal-metalloid glasses formed by combinations of late transition elements, A, with the metalloids (boron, carbon, silicon, phosphorus, or germanium), B, to compositions centering around A_4B, T_g usually increases slowly with metalloid content over the narrow composition range in which glasses readily form (*66*). This variation probably reflects the fact that the flow resistance is increased by the developing compositional SRO which attends glass formation in these alloys. However, the most conspicuous composition effect is the sharply plunging curve of T_m (at initial crystallization) with composition change, culminating in extraordinarily deep eutectics inside the composition ranges most favorable for glass formation (*67–69*). This behavior suggests that alloying affects T_{rg} primarily through its effect on T_m, so that for a particular system the lower T_m is the greater will be T_{rg} and the glass-forming tendency. Polk (*70*) suggested that the glasses with the deep eutectic compositions ($\sim A_4B$) may be relatively stabilized by the filling of the larger holes of the DRP structure of A with metalloid atoms which would fit, without severe distortions, and produce configurations similar to those in the A-rich A-B crystalline phases. Recent diffraction data (*71, 72*), which yield partial interference functions, are qualitatively consistent with such a model.

Certain alloys of late (A) with early (B) transition metals, such as copper-zirconium and nickel-niobium, also form glasses in rapid melt quenching (*3*). Further, they exhibit some intermetallic phases which melt congruently at a glass-forming composition. However, as Polk noted, the T_m's of these compounds are low compared to those (T_A and T_B) of their pure constituents.

In general, then, the A-B combinations most likely to form glasses in melt quenching are those which release large amounts of heat while forming melts with abnormally low thermodynamic crystallization temperatures. This behavior suggests (*67, 68*) a highly attractive A-B interaction, which is attenuated rather little in transition from a crystalline to an amorphous milieu. The apparent insensitivity of the A-B interaction energy to translational order seems consistent with the following hypothesis: at constant electron density, the energy of the system changes little from its minimum value with substantial dispersion of the A-B nearest-neighbor separations, r_{AB}, especially into the range where r_{AB} is well below the sum of the metallic radii ($r_A° + r_B°$) of the pure elements. Thus the numerous configurations essential for molten behavior could appear with relatively little energy increase. In support of the proposed hypothesis we note that there is, as Johnson (*73*) pointed out to us, substantial dispersion of the r_{AB}'s, and to values much below $r_A° + r_B°$, in crystalline A-B compounds. Further, it has been noted (*68*) that A-type elements are partly interstitial and diffuse by an interstitial mechanism when dissolved in certain crystalline phases of the B elements. Such interstitial solution behavior would require the occurrence of r_{AB}'s much smaller than $r_A° + r_B°$.

Little progress has been made toward a microscopic theory for the A-B interactions favorable for glass formation. However, Nagel and Tauc (*74*) made the interesting proposal that the compositions optimal for glass formation should be those at which the minima in the electronic densities of states lie at the Fermi levels. They inferred that such correspondence would confer metastability on the alloy melts. Actually, as we noted, all metallic melts are stable to temperatures far below T_m—for example, to 0.8 to 0.7 T_m. However, Nagel and Tauc may have identified one of the important liquid-stabilizing factors contributing to the lowering of T_m.

To condense a material in amorphous solid form, the condensation layer must be held at temperatures well below the kinetic crystallization temperature, T_{kc}. This temperature may be loosely defined as that at which the crystallization rate is of the order of the condensation rate. It should equal or exceed T_g when the atomic motions limiting crystal growth are like those of atomic transport within the film. We have noted that such correspondence of atomic motions should result when crystal growth is controlled by impurity redistribution. When such redistribution, in monatomic systems, is not required, the atomic shifts in crystal growth can be quite small and occur rapidly at temperatures far below T_g, relative to those in bulk atomic transport. Indeed, some metals, which crystallize when deposited in ultrapure form at temperatures as low as 4°K, will condense under similar conditions to amorphous solids with $T_{kc} > 300$°K with an impurity admixture of as little as 1 atom in 100 (*65*). In general, the condensation methods are much less constraining on the variety and range of compositions of materials that can be put into amorphous solid form than are the melt-quenching methods.

In vapor condensation of amorphous films, a stream of atoms or molecules is generated in a high-vacuum chamber, usually by heating a source material in a crucible, and deposited on some substrate at rates ranging, typically, from 1 to 10 Å/sec. These deposition rates are near the impingement rates of residual gas molecules at pressures of 10^{-5} to 10^{-6} torr. Consequently, substantial amounts of oxygen or nitrogen may be codeposited in the film unless the residual gas pressure is kept below 10^{-8} to 10^{-9} torr.

In the sputter deposition process for making amorphous films (*75*), a target of the desired composition is bombarded with atoms of a gas such as argon. Atoms from the target are ejected by this bombardment and then condensed onto a substrate. This process allows better composition control in forming multicomponent films (*56, 76*) than do other deposition processes.

Perhaps the first formation of amorphous metal films was by electrodeposition or chemical deposition from aqueous solutions (*63*). While this method is quite useful for forming relatively thick films, the difficulties of achieving conditions for codeposition of two or more alloy components limit its applicability.

In deposition processes the impingement points of atoms in the incident stream are randomly distributed. Thus a uniform coverage of the substrate is possible only if it is favored by the energetics and surface mobility of the deposited atoms. At temperatures so low that the atomic mobility on the substrate is negligible, the films grow by the formation of small clusters and their subsequent impingement. The initial nonuniformity in the oncoming stream is amplified by atomic self-shadowing and, therefore, the growing film, even though amorphous, can have anisotropic properties. Indeed, such anisotropy may be imparted deliberately by controlling the growth directionality. However, this process is still not well understood and a quantitative model for it would be useful.

In electron microscopy it is often observed that biological and polymeric materials are transformed from crystalline to amorphous forms by electron irradiation. Also, covalent crystals have been transformed into amorphous solids by ion bombardment. For example, both silicon and germanium have been made amorphous by ion implantation (*29, 77*). It appears that similar transformations of crystalline metals should be possible, but, to the best of our knowledge, they have not yet been achieved.

Properties of Metallic Glasses

The long-range periodicity of the atomic arrangement, as defined by a geometric lattice, has been extremely useful in elucidating the properties of the crystalline solid state. For example, the crystalline potential is periodic in space, and the Bloch theorem in solid-state physics is a consequence of this realization. The structure of the energy bands, which determine a variety of physical properties, is related to the symmetry properties of the lattice. Similarly, the usefulness of the reduced zone scheme relies on a periodic structure. Also, the mechanical properties of a solid are related sensitively to its structure. Indeed, a vast majority of solid-state phenomena are either directly interpretable in terms of, or related to, the crystalline lattice. We can anticipate that properties which depend on symmetry or long-range periodicity of the lattice are likely to be different in the amorphous structures. This is indeed borne out by experiments. In the following sections we summarize some of these differences, especially in metallic alloys, and comment on the technological interest in some of the outstanding properties of metallic glasses.

Electrical properties. In crystalline metallic alloys the electrical resistivity below room temperature generally decreases as the temperature decreases. This resistivity is attributed to the scattering of electrons (or holes) by phonons. As the temperature is decreased this scattering decreases, and therefore so does the resistivity. The mean free path of an electron between two scattering events is a function of temperature and can vary from a few hundred angstroms at room temperature to millimeters at low temperatures. In contrast to this behavior, the temperature dependence of the resistivity of amorphous metal alloys is rather small. Also, the sign of the temperature coefficient of electrical resistivity of amorphous metallic solids can be changed with the addition of impurities to yield a positive, zero, or negative value close to or below room temperature (*78*). Although the details of these observations are still to be explained quantitatively, several specialized applications of this behavior can be envisaged. For example, resistors made of amorphous materials can be used as standards, or they can be used in the electronics industry for thin-film applications where the short mean free path of electrons associated with compositional or positional disorder makes the amorphous materials relatively insensitive to size effects and temperature excursions above ambient. The mean free path for electrons in amorphous metallic solids is estimated to be of the order of 10 Å.

The short mean free path not only decreases the electrical conductivity in the normal state but also influences the superconducting and magnetic properties of amorphous solids. For example, when the mean free path becomes short, the superconducting coherence length decreases and the penetration depth increases in a superconductor. A material which is a type I superconductor in the crystalline state becomes a type II superconductor in the amorphous state. It follows that amorphous materials are not expected to show type I superconductivity.

Another example of the influence of a short mean free path comes from measurements of "extraordinary Hall coefficients" in amorphous alloys (*79*). The extraordinary Hall coefficients are found to be a factor of 100 larger than in the corresponding crystalline phases. This increase has been attributed to an increase in resistivity of the alloys when they have an amorphous structure. It is possible that these large extraordinary Hall coefficients will find applications as sensors for magnetic fields.

Magnetism in amorphous solids. Ferromagnetism in amorphous solids was examined theoretically by Gubanov (*80*) in 1960. Direct experimental evidence for ferromagnetism in amorphous solids, in the form of vapor-deposited films, was obtained by Mader and Nowick (*81*). Ferrimagnetism in amorphous rare earth–transition metal alloys has been observed by Orehotsky and Schroder (*82*) and by Chaudhari *et al.* (*56*). Chaudhari *et al.* also established that magnetic anisotropy can be present in amorphous alloys. The systematic investigation of amorphous magnetism in metallic alloys was accelerated by the observation of magnetic bubbles in sputtered thin-film alloys of gadolinium and cobalt and by the realization of the potential of amorphous magnetic materials in applications requiring low coercivity.

The changes in magnetic moment per atom attending a transition from a crystalline to an amorphous structure generally are of two kinds. In the rare earth–transition series, where the magnetic moment is associated with the deep inner 4*f* shells, the moment is generally not affected by a change in structure. However, in the 3*d* transition series, such as nickel, iron, and cobalt, where a band model for magnetism is more applicable, we can expect changes in moment when there is a change in the density of states. In the case of nickel and iron the moment is reduced, whereas that of cobalt is relatively unaltered (*83*).

Why the moments of nickel and iron change while that of cobalt does not is not clearly understood. It is thought that a change in the density of states in nickel plays an important role in reducing its moment. In the case of iron, the moment change may be due to the changes in coordination number, from 8 to approximately 12, and near-neighbor spacing that accompany the transition from the crystalline to the amorphous state.

Exchange interaction between magnetic atoms results in ferro- or ferrimagnetic alignment. In a perfect crystal the internal electrostatic and magnetic fields are periodic and have the same value at all equivalent structure sites. In an amorphous solid the local environment varies from point to point. For example, we expect the magnitude of the electrostatic field gradient to vary about some average value and its direction to have all possible orientations. (In reality, an amorphous solid may have some preferred direction depending on its method of fabrication.) The variation in local environment arises from fluctuations both in composition in a multicomponent system and in near-neighbor distances and coordination. A change in structure from crystalline to amorphous can therefore result in variety of changes in the overall magnetic properties of the solid. In instances where the exchange interaction is critically dependent on crystal structure, we expect the magnetic properties to be strongly perturbed in going to the amorphous structure.

Garnets are a good example of this class. Room-temperature magnetic measurements on amorphous garnets prepared by sputter deposition show no evidence of ferromagnetic behavior. However, on crystallization the same samples show ferromagnetic properties characteristic of that composition (*84*). In garnets the exchange interaction is mediated by the oxygen ions, and this requires that they be present at the correct bonding angles. Once this angle is perturbed the interaction is reduced.

Magnetic rare earth atoms (except gadolinium) have an orbital contribution to their moment which is generally not quenched by the electrostatic field gradients. However, the random variation in direction of the field gradient can result in a random variation of the direction of the orbital contribution and hence in single-ion magnetic anisotropy fluctuations. Model calculations show that these effects lower the Curie temperature and the net moment (*85*). An interesting magnetic system arises when the rare earth ions are strongly influenced by changes in direction of the crystal field. In an applied field the transition metal spins align themselves approximately parallel to the external field, whereas the rare earth ions, which couple to the transition metal ions, cannot readily do so because of the local variations in the direction of the electrostatic field gradient. An example of this class of system is an amorphous dysprosium-cobalt alloy (*86*).

In addition to the electrostatic field gradient effects on the local magnetic anisotropy, the amorphous structure can be expected to lead to a range of exchange interaction values. Mössbauer and nuclear magnetic resonance measurements show broad hyperfine field distributions rather than discrete values characteristic of crystals (*87, 88*). The Curie temperatures of amorphous magnetic alloys are generally, although not always, lower than those of their crystalline counterparts. In instances where an increase in the Curie temperature is observed, charge-transfer effects are believed to make an important contribution to the magnetic properties (*89*). At temperatures close to absolute zero, amorphous magnetic alloys show the familiar $T^{3/2}$ behavior characteristic of spin wave excitations. Spin wave modes in ferromagnetic resonance and in neutron-scattering experiments have also been reported (*90–92*). At higher temperatures the temperature dependence of magnetization can be described by a Brillouin function, although to account for the data quantitatively it may be necessary to include fluctuations in the parameters that go into the Brillouin function (*93*).

The coercivity of amorphous magnetic materials is of considerable interest both in magnetic bubble applications and in soft (low coercivity) and hard (high coercivity) magnetic applications. In the transition metal alloys the coercivity is expected to be low. The domain wall width is generally a few hundred to a few thousand angstroms. Over this distance fluctuations in compositional and structural detail in the wall will average out (*94*). In the case of rare earth–transition metal alloys, higher coercivities can be obtained because there are large local anisotropies associated with the orbital motion of the electron. Coercivities ranging from millioersteds to several thousand oersteds (*56, 76*) have been obtained in amorphous magnetic alloys. The low coercivities are of considerable interest since the amorphous alloys also have high electrical resistivities. This combination of low coercivity and high resistivity reduces the energy loss in domain wall motion and so is particularly attractive in applications where domain wall motion must occur.

We return now to the question of long-range magnetic anisotropy in liquid-quenched and vapor-deposited amorphous materials. It has been deduced that elastic stress-induced anisotrophy is present in roller-quenched iron-based alloys (*95*) and in sputtered gadolinium-iron alloys (*96*). The contribution of stress-induced anisotropy can be minimized or reduced to zero in alloys where the magnetostriction constant is small or zero. In sputtered gadolinium-cobalt alloys there is a large uniaxial anisotropy which cannot be explained on the basis of stress-induced anistropy. It is believed that there is compositional ordering in these alloys. Such ordering is the basis for a model developed by L. Néel (*96a*) and others to explain anisotropy induced in crystalline alloys by annealing in a magnetic field. It is suggested that this mechanism may also explain the induced anistropy observed in amorphous transition metal–metalloid systems when they are annealed in a magnetic field below their crystallization temperature. The compositional ordering or pair-ordering model predicts a temperature dependence of anisotropy which is in accord with experimental data (*97*). Shape effects can also give rise to magnetic anisotropy. In the case of amorphous thin films prepared by a variety of techniques, columnar growth is frequently observed. [It is likely, and in the case of cobalt-phosphorus electrodeposited films it is deduced (*98*), that this mechanism is invariably operative in deposited films.]

Understanding and control of magnetic anisotropy are crucial to virtually all applications based on magnetic phenomena. In some cases magnetic anisotropy is undesirable, whereas in others a strong uniaxial anisotropy is necessary. An example of the latter is magnetic bubbles. [These have been observed in thin-film rare earth–transition metal alloys, where, for example, bubbles with diameters of the order of 1000 Å have been observed (for example, see Fig. 4) (*99*).] The potential information packing density with such bubbles is more than 1 billion bits per square centimeter. Other storage applications can also be envisaged. The coercivity of amorphous rare earth–transition metal alloys can be tuned by judicious additions of rare earth elements with nonzero orbital moments. Video-recording media or more generally beam-addressable storage devices may be possible (*100, 101*). The soft magnetic character combined with high strength and corrosion resistance suggests that amorphous alloys may be suitable for the replacement of conventional Permalloy in certain applications. It is also conceivable that the production of wide ribbons could lead to applications in the transformer industry.

Superconductivity. Superconductivity in vapor-deposited amorphous films was reported by Bückel and Hilsch (*64*). Since then it has been observed in a variety of amorphous materials. On the theoretical side, Anderson (*102*) has shown that the Bardeen-Cooper-Schrieffer theory of superconductivity is applicable to dirty superconductors, of which amorphous superconductors might be considered a special class.

The superconducting transition temperatures of amorphous materials can be higher or lower than those of their crystalline counterparts. Collver and Hammond (*103*) have shown experimentally that the superconducting transition temperature in *d*-band amorphous transition metal alloys do not follow Matthias's rule: the peaks in the superconducting transition temperature do not occur at electron/atom ratios of 4.6 and 6.5. Instead, the amorphous *4d*-band transition metal alloys show a peak at an electron/atom ratio of 6, and the *5d*-band alloys show a peak at 7. A theory for superconductivity in amorphous transition metal alloys proposed by Kerker and Bennemann (*104*) predicts the observed superconducting transition temperatures quite well. However, the theory assumes that the change in the atomic volume when these alloys go from a crystalline to an amorphous solid structure is equal to that in melting. Experimental and theoretical evidence, at least in cases where the crystalline structure is close-packed, strongly suggests that volume changes (~ 1 to 2 percent) are actually much smaller than assumed by Kerker and Bennemann. Thus the agreement of their theory with experiment may be fortuitous. We now propose an alternative explanation.

Experience indicates that amorphous metals are 25 to 50 percent (*105*) more compliant in shear, but not appreciably in hydrostatic compression, than their crystalline counterparts. We propose that this greater shear compliance, which has been accounted for in some model calculations (*39*), will result in a 10 to 15 percent decrease in Debye temperature in the transition from close-packed crystalline to amorphous form. This decrease is sufficient to enhance the electron-phonon coupling constant and therefore increase the superconducting transition temperature. In Table 1 we list the observed and calculated values of the superconducting transition temperature, along with other data used in our calculations. In general, we expect the superconducting transition temperature to increase in amorphous metallic systems which normally have a stable crystalline structure that is close-packed.

Our assumption here is that the product of the density of states at the Fermi level and the interaction parameter is not changed in going from the crystalline to the amorphous structure in the case of close-packed structures. This assumption is consistent with the model of Barisic *et al.* (*106*), which suggests that in the transition metals this product is proportional to the cohesive energy of the solid associated with the *d*-band. We do not expect the cohesive energy to change appreciably, since the coordination number and the nearest-neighbor distance are approximately unchanged in going from the close-packed crystalline to the amorphous structure.

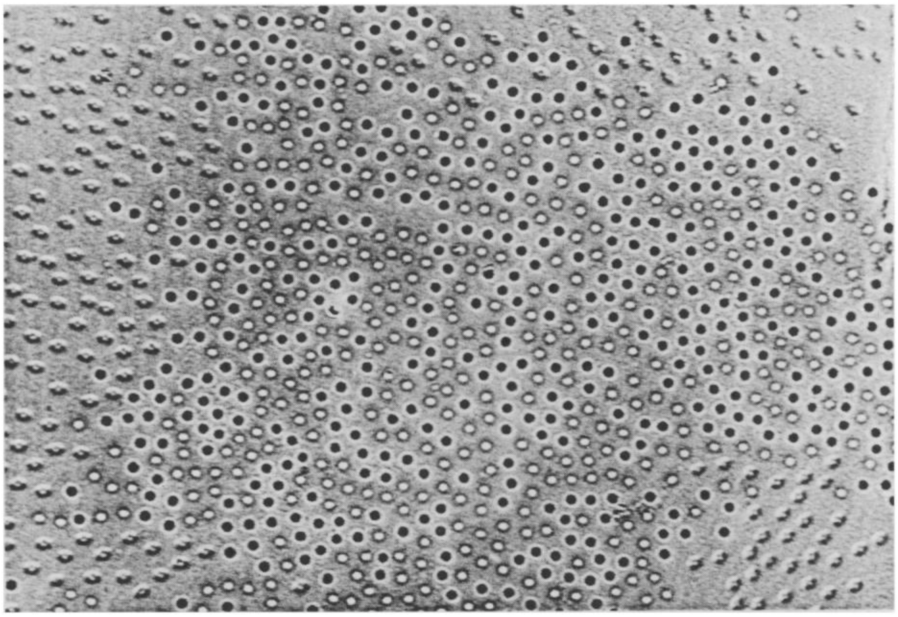

Fig. 4. Transmission electron micrograph showing magnetic bubbles in an amorphous gadolinium-cobalt alloy (*99*).

Our assumption is probably not satisfactory for transition elements such as amorphous molybdenum and niobium. Here the coordination number increases from 8 nearest neighbors of the body-centered cubic structure to a nominal 12 of the amorphous structures. It is probably even less applicable to compound superconductors such as Nb_3Ge, where a change in structure would lead to changes in bonding (*107*).

As we noted earlier, amorphous materials are expected to have the short coherence lengths and large penetration depths requisite for type II superconductors. Also, it is anticipated that the critical fields in amorphous superconductors are large. To make amorphous superconductors useful for high-field applications would require pinning of vortices. In crystalline materials this pinning may be effected by structural defects, such as grain boundaries or long dislocation lines and networks, presumably not present in alloy glasses. It is possible that effective vortex-pinning elements might be introduced into amorphous alloys by phase separation, leading to compositional inhomogeneity, or by partial crystallization. It seems to us that, considering the ease with which amorphous ribbons and wires can be fabricated, this area of application should be explored.

Considering that vortices may be able to move relatively unhindered in amorphous superconductors, we suggest that vortex storage, akin to magnetic bubble storage, should also be examined. The vortex packing density close to the second critical field is determined by the coherence length, which is estimated to be of the order of 50 Å. This length would permit a packing density of the order of 100 billion vortices per square centimeter, which is two orders of magni-

Table 1. Superconducting transition temperatures of some amorphous and crystalline metals. Symbols are defined as follows: θ_D is the Debye temperature; λ is the electron-phonon coupling constant; μ^* is the Coulomb pseudopotential; T_{exp} is the experimentally measured temperature; and $T_{cal}{}^1$ and $T_{cal}{}^2$ are temperatures calculated by using λ^1 and λ^2. The value of μ^* is taken to be the same in the amorphous and crystalline forms. In reality we expect it to decrease slightly, since the bands will smear and the density of states at the Fermi level will decrease. However, this change includes the 10 or 15 percent change in λ we have chosen. In calculating λ we have assumed that the decrease in θ_D leads to a proportional decrease in $<\omega^2<^{1/2}$, where $<\omega^2<^{1/2}$ is an average of the square of the phonon frequency. We have used the McMillan formula for calculating the transition temperatures.

Metal	Crystalline				Amorphous							
	θ_D	λ	μ^*	T_{exp}	$\theta_D{}^1$	$\theta_D{}^2$	λ^1	λ^2	μ^*	$T_{cal}{}^1$	$T_{cal}{}^2$	T_{exp}
Hafnium	252	0.34	0.13	0.09	227	214	0.42	0.47	0.13	0.49	0.94	~1.5
Iridium	420	0.34	0.13	0.14	378	357	0.42	0.47	0.13	0.82	1.56	≤1
Osmium	500	0.39	0.12	0.65	450	425	0.48	0.54	0.12	2.69	4.32	~2.75
Ruthenium	415	0.46	0.10	1.69	374	353	0.57	0.64	0.10	6.02	8.05	~7.5
Zirconium	290	0.41	0.17	0.55	261	247	0.51	0.57	0.17	0.75	1.39	~3

tude larger than the ultimate packing density for 1000-Å magnetic bubbles discussed earlier. The amorphous materials might also be useful in flux shuttle-type devices because they would allow a higher packing density.

Mechanical behavior. The mechanical behavior of metallic glasses has proved to be unexpected and quite unique. In particular, most glassy metals in their as-quenched states, at $T \ll T_g$, consistently exhibit a much higher level of tensile strength—1 to $2 \times 10^{-2}\,G$ (G is the shear modulus) or one-tenth to one-fifth the theoretical value—than do as-cast or well-annealed crystalline metals (*5, 108*). Further, and in sharp contrast with silica-based glasses, metallic glasses are appreciably ductile in tension. Their plastic response often consists of highly localized and rather large offsets on planes inclined at about 45° to the tensile axis. Also, some metallic glasses can be rolled plastically with area reductions of 80 percent. This behavior indicates toughness levels which are orders of magnitude greater than those of silica-based glasses. However, the flow stress of glassy metals, unlike that of crystalline metals, shows no measurable increase with increasing amounts of plastic deformation—that is, there is no strain hardening.

For guidance in interpreting the mechanical properties of glassy metals, we might look to the corresponding behavior of similarly composed crystalline phases. Generally, these are ordered compounds but with compositions somewhat different from those optimal for glass formation. However, their compositional order is quite similar in configuration to that thought to predominate in the corresponding glassy alloys. These compounds are hard, but unlike glassy metals they are brittle in tension. Indeed, the completely crystallized forms of glassy metals are extremely brittle and their strengths are orders of magnitude lower than those of the parent glasses.

Actually, the mechanical behavior of glassy metals appears to be somewhat similar to the "cold flow" phenomenon in glassy polymers at $T \ll T_g$ (*109*). The latter behavior is also manifested by an inhomogeneous yielding, like that in glassy metals, at similar reduced tensile strength levels, $\sim 10^{-2}\,G$.

Why the tensile responses of metallic and polymeric glasses are so different from those of glasses in which the binding is entirely covalent is a problem which has not been clearly resolved. However, it appears that the difference may have its origin in effects arising from preferred directionality in bonding. In covalently bound systems, where the interatomic forces are highly directed, configurational changes can occur only when atomic displacements are so large that the interatomic bonds are virtually broken. In a sense, the structure must be ruptured locally for any configurational change, and the stresses required for this will be so large that a microcrack, once initiated, will propagate. In systems where the bonding is largely nondirected, as in materials with metallic or van der Waals bonding, the atomic displacements which can lead to configurational rearrangements are relatively small and undirected, so they can occur at much smaller stresses than are needed for rupture. Consequently, in such systems plastic processes become available for dissipating any elastic energy concentration at the roots of microcracks.

The continuation of flow in glassy metals on the planar zone on which it was initiated suggests a flow softening; that is, the flow region has, during the offset period, less shear resistance than it initially had. Polk and Turnbull (*110*) proposed that this softening may reflect the fact that the viscosity of glassy alloys falls sharply with compositional disordering. Such disordering would attend flow while being reduced by simultaneous diffusional processes. The degree of local disorder and the corresponding viscosity would then reflect some balance between the diffusional restoration and flow rates. A quite analogous explanation for flow softening was framed in terms of the free volume model by Spaepen and Turnbull (*111*). In particular, the free volume at the leading edge of the flowing zone is increased by stress dilation with accompanying decreases in the resistances to flow and diffusion.

The mechanisms for cold flow, of either metallic or polymeric glasses, are far from clear. One mechanism derives from the free volume model (*15, 16*) developed to account for transport in simple melts. According to this model, voids form and collapse by statistical fluctuations in the local density—that is, by redistribution of the free volume. It is supposed that voids so formed may, if their volumes exceed some critical value, collapse to new local configurations. The new configurations preferred will be those which change the shape of the body in accordance with the stress bias. Thus the flow rates will be determined largely by the free volume or configuration, however produced, rather than by temperature per se. Imposition of high stresses, directly or through microcrack amplification, may increase the free volume (*111*)—"configuration excitation"—sufficiently for the occurrence of rapid local flow at temperatures far below T_g.

An alternative approach to the cold flow mechanism is in terms of the dislocation model for flow developed for crystals. Gilman (*8, 112*) has indicated how this model might be adapted to describe flow in glasses. Actually, the microscopic description is, in a certain sense, similar to that of the free volume model.

In view of their exceptionally high strength and toughness it seems that glassy metals might have important applications as structural materials, especially since their production is less complicated and more economical than that of crystalline alloys having similar high levels of mechanical performance. However, the toughness of certain glassy alloys deteriorates, by mechanisms not yet clearly understood, at temperatures well below T_g.

Surface behavior. From the time of their discovery and recognition, there has been much interest and speculation concerning the kinetic resistance of amorphous alloys to corrosive attack. From the standpoint of their supposed disorderliness, it might seem that they would be especially susceptible, in comparison with their crystallized states, to such attack. On the other hand, the DRP structure is ideally free of dislocations and intercrystalline boundaries, which are often preferred sites of chemical action. Also, as we have noted, the positions throughout this structure are highly correlated locally despite the absence of long-range translational correlation. Thus if the structures of glassy metals actually approximate the ideal DRP structure, they might prove to be exceptionally resistant to corrosion (*9*).

Several recent studies [for example, see (*113, 114*)] have indicated that late transition metal–metalloid alloys are indeed much more corrosion-resistant in their glassy than in their crystallized forms. However, these alloys, as do most glassy metals, crystallize to two or more phases with different compositions, so that it is not clear whether the superior corrosion resistance of the glasses is due to their structural or to their chemical homogeneity. It will generally be difficult to disassociate these two effects. In any event, the experiments cited are important for their indication that high degrees of homogeneity, compositional and structural, confer greatly improved corrosion resistance on alloys. Such homogeneity is probably a consequence of the rapid quenching procedures used to form glassy alloys.

References and Notes

1. P. Duwez, *Trans Am. Soc. Met.* **60**, 607 (1967); *Fizika (Zagreb) Suppl.* **2**, 1.1 (1970); *Annu. Rev. Mater. Sci.* **6**, 83 (1976).
2. T. Anantharman and C. Suryanaryana, *J. Mater. Sci.* **6**, 1111 (1971).
3. B. C. Giessen and C. N. J. Wagner, in *Physics and Chemistry of Liquid Metals*, S. Z. Beer, Ed. (Dekker, New York, 1972), pp. 633–695.
4. H. Jones, *Rep. Prog. Phys.* **36**, 1425 (1973).
5. C. A. Pampillo, *J. Mater. Sci.* **10**, 1194 (1975).
6. T. Masumoto and R. Maddin, *Mater. Sci. Eng.* **19**, 1 (1975).
7. G. S. Cargill III, *Solid State Phys.* **30**, 227 (1975).
8. J. J. Gilman, *Phys. Today* **28**, 46 (May 1975).
9. D. Turnbull, *J. Electron. Mater.* **4**, 771 (1975).
10. R. M. J. Cotterill, *Am. Sci.* **64**, 430 (1976).
11. E. U. Condon, *Am. J. Phys.* **22**, 43 (1954).
12. W. Kauzman, *Chem. Rev.* **43**, 219 (1948).
13. R. Bruckner, *J. Non-Cryst. Solids* **5**, 123 (1970).
14. K. K. Kelley and A. U. Christensen, *U.S. Bur. Mines Rep. Invest. 5710* (1961).
15. M. H. Cohen and D. Turnbull, *J. Chem. Phys.* **31**, 1164 (1959).
16. D. Turnbull and M. H. Cohen, *ibid.* **52**, 3038 (1970).
17. G. Adam and J. H. Gibbs, *ibid.* **43**, 139 (1965).
18. G. C. Berry and T. G. Fox, *Adv. Polym. Sci.* **5**, 261 (1968).
19. D. Turnbull and B. G. Bagley, in *Treatise on Solid State Chemistry*, N. B. Hannay, Ed. (Plenum, New York, 1975), vol. 5, p. 513.
20. W. H. Zachariasen, *J. Am. Chem. Soc.* **58**, 3841 (1932).
21. J. H. Gibbs and E. A. DiMarzio, *J. Chem. Phys.* **28**, 373 (1958).
22. T. W. Chapman, *Mater. Sci. Eng.* **1**, 65 (1966).
23. B. Chalmers [*Principles of Solidification* (Wiley, New York, 1964), pp. 114–116] surveys experiments of J. L. Walker and G. Colligan.
24. M. H. Cohen and D. Turnbull, *Nature (London)* **203**, 964 (1964).
25. W. Klement, R. H. Willens, P. Duwez, *ibid.* **187**, 869 (1960).
26. H. S. Chen and D. Turnbull, *J. Chem. Phys.* **48**, 2560 (1968).
27. ———, *Acta Metall.* **17**, 1021 (1969).
28. B. E. Warren, *X-ray Diffraction* (Addison-Wesley, Reading, Mass., 1969), chap. 10.
29. J. Graczyk and P. Chaudhari, *Phys. Status Solidi B* **58** 501 (1973), *J. Non-Cryst. Solids* **17**, 299 (1975).
30. D. E. Polk, *J. Non-Cryst. Solids* **5**, 365 (1971).
31. S. C. Moss and J. Graczyk, *Phys. Rev. Lett.* **23**, 1167 (1969); W. Paul, R. J. Temkin, G. A. N. Connell, *Adv. Phys.* **22**, 581 (1973).
32. O. K. Rice, *J. Chem. Phys.* **12**, 1 (1944).
33. J. D. Bernal, *Nature (London)* **185**, 68 (1960).
34. J. L. Finney, *Proc. R. Soc. London Ser. A* **319**, 497 (1970).
35. P. Chaudhari, J. F. Graczyk, D. Henderson, P. Steinhardt, *Philos. Mag.* **31**, 727 (1976); G. A. N. Connell, *Solid State Commun.* **16**, 109 (1975).
36. G. S. Cargill III, *J. Appl. Phys.* **41**, 2248 (1970).
37. ———, *ibid.*, p. 12.
38. J. F. Sadoc, J. Dixmier, A. Guinier, *J. Non-Cryst. Solids* **12**, 46 (1973).
39. D. Weaire, M. F. Ashby, J. Logan, M. J. Weins, *Acta Metall.* **19**, 779 (1971).
40. J. A. Barker, J. L. Finney, M. R. Hoare, *Nature (London)* **257**, 120 (1975); C. H. Bennett and J. L. Finney, in *Proceedings of the 2nd International Conference on Rapidly Quenched Metals,* N. J. Grant and B. C. Giessen, Eds. (MIT Press, Cambridge, Mass., 1976), sect. 1, p. 231; G. S. Cargill and S. Kirkpatrick, *AIP Conf. Proc. No. 31* (1976), p. 3.
41. F. C. Frank, *Proc. R. Soc. London Ser. A* **215**, 43 (1952).
42. ——— and J. S. Kasper, *Acta Crystallogr.* **11**, 184 (1958).
43. M. R. Hoare and P. Pal, *Adv. Phys.* **24**, 645 (1975).
44. C. L. Briant and J. J. Burton, *J. Chem. Phys.* **63**, 2045 (1975).
45. L. W. Tilton, *J. Res. Natl. Bur. Stand.* **59**, 139 (1957).
46. R. Grigorivici and R. Manaila, *Thin Solid Films* **1**, 343 (1968).
47. J. Farges, M. F. DeFeraudy, B. Raoult, G. Torchet, *J. Phys. (Paris)* **36**, C2 (1975).
48. C. H. Bennett, *J. Appl. Phys.* **43**, 2727 (1972).
49. D. J. Adams and A. J. Matheson, *J. Chem. Phys.* **56**, 1989 (1972).
50. M. L. Rudee, *Phys. Status Solidi B* **46**, K1 (1971).
51. P. Chaudhari, J. F. Graczyk, S. Herd, *ibid.* **51**, 801 (1972).
52. M. L. Rudee and A. Howie, *Philos. Mag.* **25**, 1001 (1972); A. Howie, O. L. Krivanek, M. L. Rudee, *ibid.* **27**, 235 (1973).
53. S. Herd and P. Chaudhari, *Phys. Status Solidi A* **26**, 627 (1974).
54. R. Geiss, in *Developments in Electon Microscopy and Analysis*, J. A. Venables, Ed. (Academic Press, New York, 1976), p. 61.
55. J. Graczyk and P. Chaudhari, *Phys. Status Solidi B* **75**, 593 (1976); R. Alben, G. S. Cargill III, and J. Wenzel [*Phys. Rev. B* **13**, 835 (1976)] have also analyzed the DRP model.
56. P. Chaudhari, J. J. Cuomo, R. J. Gambino, *IBM J. Res. Dev.* **17**, 66 (1973).
57. D. Henderson, M. Brodsky, P. Chaudhari, *Appl. Phys. Lett* **25**, 11 (1974).
58. D. Turnbull, in *Physics of Non-Crystalline Solids*, J. W. Prins, Ed. (North-Holland, Amsterdam, 1964), pp. 41–56.
59. ———, *Contemp. Phys.* **10**, 473 (1969).
60. D. R. Uhlmann, *J. Non-Cryst. Solids* **7**, 337 (1972).
61. H. A. Davies and B. G. Lewis, in *Proceedings of the 2nd International Conference on Rapidly Quenched Metals*, N. J. Grant and B. C. Giessen, Eds. (MIT Press, Cambridge, Mass., 1976), sect. 1, p. 259.
62. F. Spaepen and D. Turnbull, in *ibid.*, p. 205.
63. A. Brenner, D. E. Couch, E. K. Williams, *J. Res. Natl. Bur. Stand.* **44**, 109 (1950).
64. W. Bückel and R. Hilsch, *Z. Phys.* **138**, 109 (1954).
65. B. Schroeder *et al.*, *AIP Conf. Proc. No. 31* (1976), p. 353; J. C. Suits, *Phys. Rev.* **134**, 588 (1963).
66. See, for example, H. S. Chen, *Acta Metall.* **22**, 1505 (1974).
67. M. H. Cohen and D. Turnbull, *Nature (London)* **189**, 131 (1961).
68. D. Turnbull, *J. Phys. (Paris) Colloq. 4* **35**, 1 (1974).
69. M. Marcus and D. Turnbull, *Mater. Sci. Eng.* **23**, 211 (1976).
70. D. E. Polk, *Acta Metall.* **20**, 485 (1972).
71. J. Dixmier, J. Bletry, J. F. Sadoc, *J. Phys. (Paris)* **36**, C2 (1975); J. Bletry and J. F. Sadoc, *J. Phys. F* **5**, L110 (1975).
72. Y. Waseda and N. Tamaki, *Z. Phys. B* **23**, 315 (1976).
73. W. L. Johnson, personal communication.
74. S. R. Nagel and J. Tauc, *Phys. Rev. Lett.* **35**, 380 (1975).
75. K. L. Chopra, *Thin Film Phenomena*, (McGraw-Hill, New York, 1969), p. 196.
76. J. J. Rhyne, S. J. Pickart, H. A. Alperin, *Phys. Rev. Lett.* **29**, 1562 (1972).
77. J. Smith, M. Brodsky, W. Crowder, M. Nathan, A. Pinczuk, *ibid.* **26**, 642 (1971).
78. R. Hasegawa and C. C. Tsuei, *Phys. Rev. B* **2**, 1631 (1970).
79. S. C. M. Lin, *J. Appl. Phys.* **40**, 2175 (1969); K. Okamoto, T. Sirokawa, S. Matsushita, Y. Sakurai, *IEEE Trans. Magn.* **MAG-10**, 799 (1976); T. R. McGuire, R. J. Gambino, R. Raylor, *J. Appl. Phys.*, in press.
80. A. I. Gubanov, *Sov. Phys. Solid State* **2**, 468 (1960).
81. S. Mader and A. S. Nowick, *Appl. Phys. Lett.* **7**, 57 (1965).
82. J. Orehotsky and K. Schroder, *J. Appl. Phys.* **43**, 2413 (1972).
83. J. G. Wright, paper presented at the 7th International Colloquium on Magnetic Thin Films, Regensburg, West Germany, April 1975.
84. J. J. Cuomo, V. Sadagopan, J. DeLuca, P. Chaudhari, R. Rosenberg, *Appl. Phys. Lett.* **12**, 581 (1972).
85. R. Harris, M. Plischke, M. J. Zuckermann, *Phys. Rev. Lett.* **31**, 160 (1973); D. Sarkar, R. Segman, E. K. Cornell, E. Callen, R. Harris, M. Plischke, M. J. Zuckermann, *ibid.* **32**, 542 (1974).
86, J. M. D. Coey, J. Chappert, J. P. Rebouillat, T. S. Wang, *ibid.* **36**, 1061 (1976).
87. T. E. Sharon and C. C. Tsuei, *Phys. Rev. B* **5**, 1047 (1972); N. Heiman and K. Lee, *Phys. Lett. A* **55**, 297 (1975), D. W. Forester, *AIP Conf. Proc. No. 31* (1976), p. 384.
88. K. Raj. J. I. Budnick, R. Alben, G. C. Chi, G. S. Cargill, *AIP Conf. Proc. No. 31* (1976), p. 390; J. Durand, *J. Phys. F*, in press.
89. L. J. Tao, S. Kirkpatrick, R. J. Gambino, J. J. Cuomo, *Solid State Commun.* **13**, 1491 (1973).
90. T. Mizoguchi, *AIP Conf. Proc. No. 34* (1976), p. 286.
91. J. R. McGoll, D. Murphy, G. S. Cargill III, T. Mitzoguchi, *AIP Conf. Proc. No. 29* (1976), p. 172.
92. J. D. Axe, L. Passell, C. C. Tsuei, *AIP Conf. Proc. No. 24* (1975), p. 119.
93. C. C. Tsuei and H. Lillenthal, *Phys. Rev. B* **13**, 4899 (1976).
94. D. I. Paul, in *Proceedings of the 2nd International Conference on Amorphous Magnetism*, R. A. Levy and R. Hasegawa, Eds. (Plenum, New York, 1977), p. 403.
95. E. E. Luborsky, J. L. Walter, D. E. LeGrand, *IEEE Trans. Magn.* **MAG-12**, 930 (1976).
96. R. Zwingmann, W. C. Wilson, Jr., H. C. Bourne, Jr., *AIP Conf. Proc. No. 34* (1976), p. 334.
96a. L. Néel, *C.R. Acad. Sci.* **225**, 109 (1947).
97. P. Chaudhari and D. C. Cronemeyer, *AIP Conf. Proc. No. 29* (1976), p. 113.
98. G. C. Chi and G. S. Cargill III, *ibid.*, p. 147.
99. P. Chaudhari and S. Herd, *IBM J. Res. Dev.* **20**, 102 (1976).
100. P. Chaudhari, J. J. Cuomo, R. J. Gambino, *Appl. Phys. Lett.* **22**, 337 (1973).
101. K. Sunago, S. Matsushita, Y. Sakurai, *IEEE Trans. Magn.* **MAG-12**, 776 (1976); Y. Mimamura, N. Imamura, T. Kobayashi, *ibid.* p. 779.
102. P. W. Anderson, *J. Phys. Chem. Solids* **11**, 26 (1959).
103. M. M. Collver and R. H. Hammond, *Phys. Rev. Lett.* **30**, 92 (1973).
104. G. Kerker and K. H. Bennemann, *Z. Phys.* **264**, 15 (1973).
105. See, for example, the review article by B. S. Berry, in *Metallic Glasses*, J. J. Gilman and H. J. Leamy, Eds. (American Society for Metals, Cleveland, in press).
106. S. Barisic, J. Labbe, J. Friedel, *Phys. Rev. Lett.* **25**, 919 (1970).
107. R. Pollak, C. C. Tsuei, R. W. Johnson, *Solid State Commun.*, in press.
108. L. A. Davis, in *Proceedings of the 2nd International Conference on Rapidly Quenched Metals*, N. J. Grant and B. C. Giessen, Eds. (MIT Press, Cambridge, Mass., 1976), sect. 1, p. 369.
109. A. Argon, in *Polymeric Materials*, E. Baer and S. V. Radcliffe, Eds. (American Society for Metals, Cleveland, 1975), pp. 411–485.
110. D. E. Polk and D. Turnbull, *Acta Metall.* **20**, 493 (1972).
111. F. Spaepen and D. Turnbull, *Scripta Metall.* **8**, 563 (1974).
112. J. J. Gilman, *J. Appl. Phys.* **44**, 675 (1973).
113. R. B. Dingle and J. E. Slater, *Corrosion* **32**, 155 (1976).
114. K. Hashimoto and T. Masumoto, *Mater. Sci. Eng.* **23**, 285 (1976).

Copying License for Material from *Science*

Readers of *Science* who require copies of papers beyond the numbers permitted under the "fair use" provisions of the new copyright law may purchase reprints, obtain permission to copy the paper direct from AAAS, or make use of a general copying license provided through the Copyright Clearance Center, Inc. (see pages 10 and 32). Materials licensed through the Copyright Clearance Center are identified by a code that appears in the middle of the folio line on the first page of each article (see page 22). The first eight digits of the code are the International Standard Serial Number assigned to *Science*. The next two digits identify the year. The next eight digits, in two sets of four, identify the issue date and page number. The last four show the copying fee for the article. Librarians and others who wish to use the services of the Copyright Clearance Center may obtain information from the Center, 1 Park Avenue, New York, N.Y. 10016.